J. Soil Groundwater Environ. Vol. 27(6), p. 11~21, 2022
https://doi.org/10.7857/JSGE.2022.27.6.011
≪ Research Paper ≫
ISSN 1598-6438 (Print), ISSN 2287-8831 (Online)

Single and Binary Competitive Sorption of Phenanthrene and Pyrene in Natural and Synthetic Sorbents

Md Abdullah Al Masud · Won Sik Shin*

School of Architecture, Civil, Environmental and Energy Engineering, Kyungpook National University, Daegu 41566, Republic of Korea

ABSTRACT

Sorption of phenanthrene (PHE) and pyrene (PYR) in several sorbents, i.e., natural soil, BionSoil®, Pahokee peat, vermicompost and Devonian Ohio Shale and a surfactant (hexadecyltrimethyl ammonium chloride)-modified montmorillonite (HDTMA-M) were investigated. Pyrene exhibited higher sorption tendency than phenanthrene, as predicted by its higher octanol to water partition coefficient (K_{ow}). Several sorption models: linear, Freundlich, solubility-normalized Freundlich model, and Polanyi-Manes model (PMM) were used to analyze sorption isotherms. Linear isotherms were observed for natural soil, BionSoil®, Pahokee peat, vermicompost, while nonlinear Freundlich isotherms fitted for Ohio shale and HDTMA-M. The relationship between sorption model parameters, organic carbon content (f_{oc}), and elemental C/N ratio was studied. In the binary competitive sorption of phenanthrene and pyrene in natural soil, competition between the solutes caused reduction in the sorption of each solute compared with that in the single-solute system. The ideal adsorbed solution theory (IAST) coupled with the single-solute Freundlich model was not successful in describing the binary competitive sorption equilibria. This was due to the inherent nature of linear sorption of phenanthrene and pyrene in natural soil. The result indicates that the applicability of IAST for the prediction of binary competitive sorption is limited when the sorption isotherms are inherently linear.

Key words : Competition, Phenanthrene, Pyrene, Sorption, Sorbent

1. Introduction

Polycyclic aromatic hydrocarbons (PAHs) with several aromatic rings are commonly derived from inadequate combustion of raw materials in the coal and petrochemical industries, automotive exhaust emissions, and leakage of oil products. Because of their high toxicity and durability, the US Environmental Protection Agency (EPA) reported that PAHs are major pollutants in groundwater and soil (Krzyszczak et al., 2022). PAHs have been sustained in the environment for a long time and are extremely resistant to natural degradation processes because of their low biodegradability, weak ionization capacity, low water solubility (Zhu et al., 2016). The incidence of PAHs pollution in the environment has significantly increased in recent decades. Furthermore, PAHs must be rapidly removed from the aquatic environment because they build up in living tissues and have been linked to a variety of diseases and concerns in humans (Luna et al., 2016). PAHs have been removed from aqueous and solid systems using a variety of techniques, including adsorption, flocculation, coagulation, membrane filtration, solvent extraction, biological treatment and advanced oxidation processes (AOPs) (Akinpelu et al., 2019; Al-Masud et al., 2022a; Masud et al., 2022; Niasar et al., 2016; Nyström et al., 2020; Pathak et al., 2022). However, the types of adsorbents are crucial for the effectiveness of adsorption toward particular pollutants.

The competitive adsorption of organic compounds in multi-solute systems has been predicted using the ideal adsorbed solution theory (IAST). IAST has the advantages that no mixture data are required and no restriction exists for the type of pure-component isotherm equation (Qiao and Hu, 2000), but IAST can make erroneous predictions caused by a large difference in molecular size and adsorbent heterogeneity (Oh et al., 2009). To overcome this drawback,

주저자: Md Abdullah Al Masud, 박사과정
*교신저자: Won Sik Shin, 교수
Email: wshin@knu.ac.kr

Received : 2022. 11. 04 Reviewed : 2022. 11. 14
Accepted : 2022. 11. 23 Discussion until : 2023. 02. 28

many studies on IAST have been carried out (Chen et al., 2022; Papageorgiou et al., 2009). Although several thermodynamic competitive sorption models such as ideal adsorbed solution theory (IAST) and competitive Langmuir model (CLM) have been used for understanding and predicting competitive sorption of multi-solutes, little information is currently available for sediments (Oh et al., 2009).

This study may lead to a better understanding of the mechanistic explanation of PAHs' sorption behavior in natural soil environments. In this study examines the details of the adsorption of PAHs (phenanthrene and pyrene) on six different sorbents, i.e., natural soil, BionSoil®, Pahokee peat, vermicompost and Devonian Ohio Shale and a surfactant (hexadecyltrimethyl ammonium chloride)-modified montmorillonite (HDTMA-M) soil through batch experiments. Linear, Freundlich, Solubility-normalized Freundlich, Polanyi-Manes (PM), and binary competitive sorption models were applied to fit the sorption isotherms. The objectives of this study were to (1) compare the adsorption of phenanthrene and pyrene; (2) compare the sorption of different sorbents; and (3) compare different models for sorption with sorbents.

2. Materials and Method

2.1. Chemicals

^{14}C-radiolabeled phenanthrene (PHE, ARC, 53.2 Ci/mol, >99%)) and pyrene (PYR, ChemSyn Laboratories, 53.2 Ci/mol, >99.95%), were used as radiotracers, purchased from Sigma-Aldrich Chemical Co. Physicochemical properties of PHE and PYR are listed in Table S1. As a bacterial inhibitor, 200 mg/L of NaN_3 was added to the solution. Before each sorption experiment, solutions were prepared by mixing ^{12}C stock solutions with an electrolyte solution containing 1 mM $CaCl_2{\cdot}2H_2O$, 0.5 mM $MgCl_2$, and 1 mM $Na_2B_4O_{10}{\cdot}H_2O$ (pH 7.0). All chemicals were used without further purification.

2.2. Sorbents

Six different sorbents: Pahokee peat (International Humic Substances Society, St. Paul, MN, USA), BionSoil® (Bion Environmental Technologies, Inc., USA), vermicompost (or earthworm casting) from a food waste composting industry (Eco Biotech, Kyunggi-Do, Korea), Devonian Ohio shale (USGS, Denver, CO, USA), a natural soil collected from a local horizon near Daegu, Korea, and montmorillonite-KSF (Aldrich) modified with a cationic surfactant, hexadecyl trimethyl-ammonium (HDTMA) to 50% of the CEC of the montmorillonite (50% HDTMA-M) were used in this study. 50% HDTMA-M was prepared by following the procedure by Kim et al. (1996) (Kim et al., 1996). Soil samples were air-dried and sieved through 850 μm (200 × 25 mm mesh size, USA) before use. The sorbent properties were determined by Huffmann Laboratories, Inc. (Golden, CO, USA) and are summarized in Table S2.

2.3. Experiment methods

Batch sorption experiments were conducted at 25°C in 40 mL amber glass vials (Fisher Co.) with open-top polypropylene screw thread caps and Teflon-faced silicon septa (Kimble Chase, USA). Control experiments were conducted to investigate the sorption of chemicals on the surface of the glassware, and the results showed that sorption of PHE and PYR on the glass surfaces was negligible. To obtain sorption isotherms, seven different initial concentrations (0.05 mg/L to 1 mg/L for PHE and 0.005 mg/L to 0.1 mg/L for PYR) of each compound were used. The headspace in the vials was kept to a minimum after filling with sorbent and spiking solutions. The sorbent/water mixture was horizontally mixed in a shaker bath at a 25°C temperature. After 2 days of mixing, the sorbent was separated from the solution by centrifugation at 2,500 rpm for 20 min, and the residue concentration in the supernatant was analyzed by a liquid scintillation counter (LSC, EG &G Wallac Co., 1220 Quantulus). The solid phase equilibrium concentrations were calculated by assuming all concentration changes in the solution phase resulted from sorption onto the solid phase. All sorption experiments were conducted in duplicate.

Binary solutions (^{14}C-phenanthrene/^{12}C-pyrene or ^{12}C-phenanthrene/^{14}C-pyrene) were prepared by mixing each PAH solution at the same mass concentration in a 1:1 volume ratio, resulting in seven different initial concentrations (from 0.0025 to 0.1 mg/L) for each solute. Binary sorption experiments were conducted in the same manner as single sorption experiments. The equilibrium concentrations in the mixture were also determined by LSC. The sorption and desorption model parameters were determined by using a commercial software package, Table Curve 2D® (Version 5.1, Systat, Inc.).

2.4. Application of Adsorption Models

2.4.1. Linear Model

The linear sorption model is defined in equation (1):

$$q = K_d C = K_{oc} f_{oc} C \quad (1)$$

where q (mg/g) = the equilibrium concentration in the solid phase, K_d (L/g) = the linear distribution coefficient, C (mg/L) = the equilibrium concentration in the solution phase and K_{oc} (L/g OC) = organic carbon normalized partition coefficient and f_{oc} = organic carbon content.

2.4.2. Freundlich Model

Freundlich model was also used to fit the single-solute sorption in equation (2):

$$q = K_F C^{N_F} = K_{F,oc} f_{oc} C^{N_F} \quad (2)$$

where K_F [(mg/kg)/(mg/L)^N] and N_F (dimensionless) are the Freundlich sorption coefficient and the Freundlich exponent, respectively and $K_{F,oc}$ [(mg/kg OC)/(mg/L)^N] is the organic carbon normalized Freundlich sorption coefficient (Al-Masud et al., 2023).

2.4.3. Solubility-normalized Freundlich Model

In this study, a solubility-normalized Freundlich model was used to fit the single-solute sorption in equation (3) (Shin and Song, 2005):

$$q = K'_F \left(\frac{C}{S_w}\right)^{N_F} = K'_{F,oc} f_{oc} \left(\frac{C}{S_w}\right)^{N_F} \quad (3)$$

where S_w (mg/L) is the solute's aqueous solubility, K'_F (mg/g) is the unit-normalized Freundlich sorption coefficient and $K'_{F,oc}$ (mg/kg OC) is organic carbon normalized form of K'_F. The use of C/S_w yields that K'_F values are independent of the values of N. In Eq. (3), K'_F has the same units as q and its magnitude is equal to the value of q at $C/S_w = 1$. Thus K'_F represents the mass of HOC sorbed per unit mass of sorbent when the C approaches saturation ($C \rightarrow S_w$), regardless of the units of C. This approach implicates that the unit-normalized Freundlich sorption coefficient (K'_F) has both physical significance and meaningful units in addition to providing a flexible choice of units for C.

2.4.4. Polanyi-Manes Model (PMM)

A sorption model based on Polanyi-Mane's theory in equation (4) was used to fit sorption data:

$$q = q_{\max} \exp\left\{-\alpha\left(\frac{\varepsilon_{sw}}{V_m}\right)^{\beta}\right\} = q_{\max} \exp\left\{-\alpha\left(\frac{RT\ln(S_w/C)}{V_m}\right)^{2}\right\} \quad (4)$$

where q_{max} is the maximum sorption capacity (mg/kg), α and β are fitting parameters, V_m is the molar volume of the solute (L/mol) and ε_{sw} is the Polanyi's adsorption potential ($= RT \ln (S_w / C)$). For $\beta = 2$, the Dubinin-Radushkevich equation is obtained. In this study, β was fixed to be 2 to decrease the number of parameters to be estimated (Kleineidam et al., 2002).

2.4.5. Binary Competitive Sorption Model

Ideal adsorbed solution theory (IAST) was applied to model binary competitive sorption of PHE/PYR in natural soil. IAST is based on the equivalence of spreading pressure in a mixture under equilibrium. The equivalence of spreading pressure in a mixture containing N solutes leads to equations (5-7) (Choi and Shin, 2020; Kim et al., 2005).

$$\pi = \frac{RT}{A}\int_0^{q_1^*}\frac{d\log C_1}{d\log q_1}dq_1 = \frac{RT}{A}\int_0^{q_2^*}\frac{d\log C_2}{d\log q_2}dq_2 = \cdots = \frac{RT}{A}\int_0^{q_N^*}\frac{d\log C_N}{d\log q_N}dq_N \quad (5)$$

or

$$\pi = \frac{RT}{A}\int_0^{C_1^*}\frac{q_1}{C_1}dq_1 = \frac{RT}{A}\int_0^{C_2^*}\frac{q_2}{C_2}dq_2 = \cdots = \frac{RT}{A}\int_0^{C_N^*}\frac{q_N}{C_N}dq_N \quad (6)$$

Other equations involved in IAST calculation are:

$$C_{m,i} = z_i C_i^*,\ \sum_{i=1}^{N} z_i = 1,\ q_i^* = f(C_i^*),\ \frac{1}{q_T} = \sum_{i=1}^{N}\frac{z_i}{q_i^*},\ q_{m,i} = z_i q_T = q_{m,i}^0 + \frac{V(C_{m,i}^0 - C_{m,i})}{W} \quad (7)$$

In the above equations, $C_{m,i}$ and $q_{m,i}$ are equilibrium concentration in the liquid phase and in the sorbed phase of a solute i in a mixture, respectively. Superscript 0 in these variables represent initial concentration in N-solute sorption. z_i represents the mass fraction of solute i in the sorbed phase, and C_i^* and q_i^* refer to equilibrium concentrations in the liquid and solid phases of solute i that sorbs singly from solution at the same temperature and spreading pressure as those of the mixture, respectively. The function f in $q_i^* = f(C_i^*)$ denotes a single-solute sorption model for solute i. q_T is the total sorbed concentration of all solutes in the mixture. V and W represent the solution volume and sorbent weight, respectively. There are $5N$+1 equations in total, while $C_{m,i}$, $q_{m,i}$, C_i^*, q_i^*, z_i, and q_T comprise a set of $5N$+1 unknowns. Therefore, it can predict the multi-solute sorption data, $q_{m,i}$ vs. $C_{m,i}$, by solving these equations simultaneously. A Fortran program was written to calculate competitive sorption equilibria. The IAST calculations were conducted in molar units and converted to mass units for graphical representations.

3. Results and discussion

3.1. Single-Solute Sorption

Single-solute sorption of PHE and PYR to several sorbents were presented in Fig. 1 and Fig. 2, respectively. Apparently,

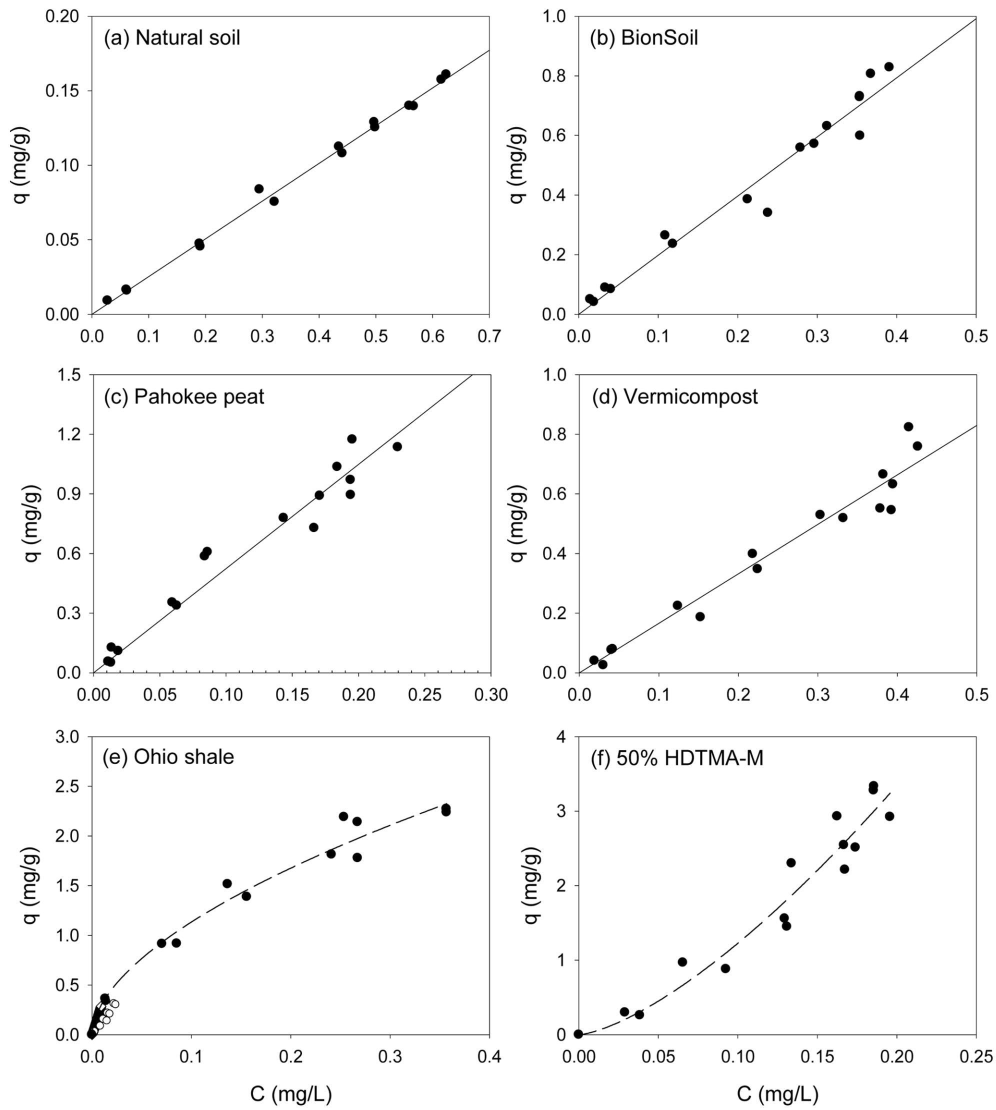

Fig. 1. Sorption isotherms of phenanthrene in several sorbents. (a) natural soil (0.1 g), (b) BionSoil® (0.03 g), (c) Pahokee peat (0.03 g), (d) worm casting (0.03 g), (e) Ohio shale (0.01 g) and (f) 50% HDTMA-M (0.01 g). Note changes in scale.

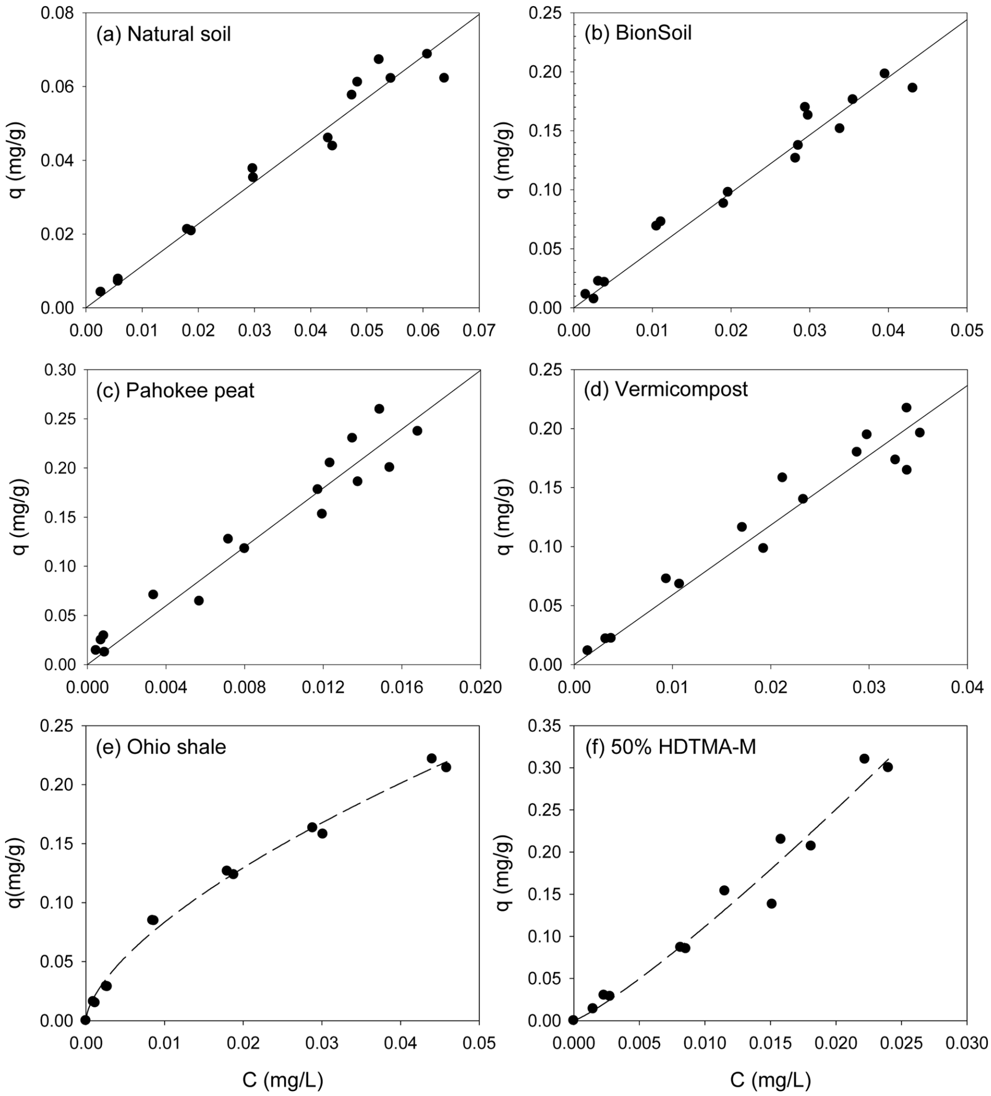

Fig. 2. Sorption isotherms of pyrene in several sorbents. (a) natural soil (0.02 g), (b) BionSoil® (0.01 g), (c) Pahokee peat (0.01 g), (d) worm casting (0.01 g), (e) Ohio shale (0.01 g) and (f) 50% HDTMA-M (0.01 g). Note changes in scale.

sorption isotherms of the PAHs were linear in natural soil, BionSoil®, Pahokee peat and vermicompost, but nonlinear in Ohio shale and 50% HDTMA-M. The model parameters of linear, Freundlich, solubility-normalized Freundlich, and PM models were listed in Tables 1, 2, and 3, respectively.

3.1.1. Linear model

As listed in Table 1, the linear isotherm model is well-fitted with the coefficient of determination ($R^2 > 0.90$) for the all sorbents and both PHE and PYR. The partition coefficient (K_d) of PYR was higher than PHE for natural soil, BionSoil®, Pahokee peat, and vermicompost sorbents, except Ohio Shale and 50% HDTMA-M.

The K_d increased linearly as f_oc and C/N ratio increased ($R^2 > 0.94$) except Ohio shale and 50% HDTMA-M. The log K_{oc} values were in the order of 50% HDTMA > Ohio Shale > BionSoil® > vermicompost > Pahokee peat > natural soil, except PYR in Ohio shale (Table 1). The log K_{oc} values of sorbents were less than the log K_{ow} values of phenanthrene (~ 4.46) and pyrene (~ 4.88) except Ohio shale and 50% HDTMA-M. Similar results were observed by Barriuso at al., (1992) (Barriuso et al., 1992). They showed that K_{oc} values for soils with high organic carbon contents are usually lower than K_{ow} value, compared to the soils with

Table 1. Linear sorption parameters for sorption of phenanthrene and pyrene in sorbents. (K_{oc} = organic carbon normalized partition coefficient)

Sorbent	Sorbate	K_d [a]	K_{oc} [b]	log K_{oc}	SAR	R^2	SSE
Natural soil	PHE	0.253 ± 0.002	11.25 ± 0.10	4.051	1.0	0.9958	0.0002
	PYR	1.137 ± 0.028	50.52 ± 1.26	4.703	1.0	0.9665	0.0003
BionSoil®	PHE	1.983 ± 0.052	17.84 ± 0.47	4.251	7.8	0.9635	0.0435
	PYR	4.886 ± 0.133	43.94 ± 1.92	4.643	4.3	0.9593	0.0027
Pahokee peat	PHE	5.243 ± 0.164	11.47 ± 0.36	4.059	21	0.9484	0.1214
	PYR	14.96 ± 0.506	32.72 ± 1.11	4.515	13	0.9410	0.0066
Vermicompost	PHE	1.659 ± 0.050	12.11 ± 0.37	4.083	6.6	0.9537	0.0492
	PYR	5.915 ± 0.196	43.18 ± 1.43	4.635	5.2	0.9343	0.0044
Ohio Shale	PHE	7.336 ± 0.404	75.78 ± 4.18	4.880	29	0.9510	1.1300
	PYR	5.328 ± 0.272	55.04 ± 2.81	4.741	4.7	0.9206	0.0040
50% HDTMA-M	PHE	15.23 ± 0.660	275.44 ± 11.94	5.440	60	0.9035	1.7500
	PYR	12.33 ± 0.428	223.03 ± 7.74	5.348	11	0.9669	0.0052

Units: K_d = (mg/g)/(mg/L) and K_{oc} = (mg/g OC)/(mg/L).

Table 2. Freundlich and solubility-normalized Freundlich model parameters for sorption and desorption of phenanthrene and pyrene in sorbents. ($K_{F,oc}$ and $K'_{F,oc}$ = organic carbon normalized Freundlich and solubility-normalized Freundlich coefficient, respectively)

Sorbent	Solute	K_F	N_F	$K_{F,oc}$	K'_F	$K'_{F,oc}$	R^2	SSE
Natural soil	PHE	0.253 ± 0.006	0.9975 ± 0.032	11.23 ± 0.27	0.2905 ± 0.0082	12.91 ± 0.36	0.995	0.0002
	PYR	0.860 ± 0.203	0.9077 ± 0.077	38.24 ± 9.02	0.1397 ± 0.0116	6.21 ± 0.52	0.969	0.0003
BionSoil®	PHE	2.186 ± 0.281	0.9854 ± 0.111	19.66 ± 2.53	2.5441 ± 0.3657	22.88 ± 3.29	0.964	0.0419
	PYR	2.870 ± 0.701	0.8456 ± 0.070	25.81 ± 6.31	0.5279 ± 0.0558	4.75 ± 0.50	0.969	0.0021
Pahokee peat	PHE	3.942 ± 0.577	0.8366 ± 0.091	8.30 ± 1.26	4.4313 ± 0.6980	9.70 ± 1.53	0.958	0.0965
	PYR	9.317 ± 4.573	0.8908 ± 0.112	20.39 ± 10.01	1.5653 ± 0.4171	3.43 ± 0.91	0.944	0.0062
Vermicompost	PHE	1.788 ± 0.229	1.0726 ± 0.121	13.06 ± 1.67	2.0778 ± 0.3004	21.47 ± 3.10	0.954	0.0480
	PYR	3.335 ± 1.125	1.1250 ± 0.093	24.34 ± 8.21	0.6215 ± 0.0941	6.42 ± 0.97	0.945	0.0037
Ohio Shale	PHE	4.158 ± 0.307	0.5643 ± 0.049	42.95 ± 3.18	4.4989 ± 0.3632	32.84 ± 2.65	0.973	0.2020
	PYR	1.553 ± 0.146	0.6349 ± 0.026	16.04 ± 1.51	0.4355 ± 0.0186	3.18 ± 0.14	0.993	0.0005
50% HDTMA-M	PHE	34.19 ± 12.59	1.4452 ± 0.204	618.34 ± 227.64	41.85 ± 16.62	756.78 ± 300.47	0.933	1.1988
	PYR	24.25 ± 10.23	1.1687 ± 0.105	438.59 ±184.92	2.3356 ± 0.4940	42.24 ± 8.93	0.973	0.0042

Units: K_F = [(mg/g)/(mg/L)^N], N = dimensionless, K'_F = mg/g, and $K'_{F,oc}$ = mg/g OC.

'normal' and very low organic carbon contents. The K_{oc} values of PYR were higher than those of PHE indicating higher sorption affinity of PYR due to its higher hydrophobicity.

3.1.2. Freundlich isotherm model

The sorption data of five different sorbents were fitted using the Freundlich model, and model parameters and fitting results are summarized in Table 2. As indicated by the high R^2 values (> 0.93), the Freundlich model better describes the adsorption process. The well-fitted adsorption process with the high regression coefficient (R^2 = 0.933-0.995) of all sorbents indicates the possibility of multilayer adsorption (Shakya et al., 2022).

The Freundlich sorption coefficient, K_F, indicates the sorption capacity of the sorbent. The Freundlich coefficient (K_F) of PHE was in the order of 50% HDTMA-M (34.19) > Ohio Shale (4.15) > Pahokee peat (3.94) > BionSoil® (2.18) > vermicompost (1.78) > natural soil (0.25). The Freundlich coefficient (K_F) was in the order of 50% HDTMA-M (24.25) > Pahokee peat (9.13) > vermicompost (3.33) > BionSoil® (2.87) > Ohio Shale (1.55) > natural soil (0.86) for PYR.

The Freundlich exponent (N_F), is a measure of the deviation from linearity of the sorption. According to the Freundlich theory, the adsorption isotherm becomes linear when N_F = 1, favorable when N_F < 1, and unfavorable when

$N_F > 1$. Moreover, the significance of the N_F value for the adsorption of PHE and PYR onto the natural soil, BionSoil®, Pahokee peat, and Ohio Shale is a chemical process ($N_F < 1$) and vermicompost and 50% HDTMA-M is a physical process ($N_F > 1$) (Tran et al., 2017).

3.1.3. Solubility-normalized Freundlich model

The results of solubility-normalized Freundlich model analysis were listed in Table 2. The solubility-normalized Freundlich coefficient (K'_F) was in the order of 50% HDTMA-M (41.85) > Ohio Shale (4.49) > Pahokee peat (4.43) > BionSoil® (2.54)> vermicompost (2.07) > natural soil (0.29) > for PHE. In PYR sorption, the order was 50% HDTMA-M (2.33) > Pahokee peat (1.56) > vermicompost (0.62) > BionSoil® (0.52) > Ohio Shale (0.43) > natural soil (0.13). The organic carbon normalized solubility-normalized Freundlich coefficient ($K'_{F,oc}$) was in the order of 50% HDTMA-M (756.78)) > Ohio Shale (32.84) > BionSoil® (22.88) > vermicompost (21.47) > natural soil (12.91) > Pahokee peat (9.7) for PHE. For pyrene, $K'_{F,oc}$ was in the order of 50% HDTMA-M (42.24) > vermicompost (6.42) > natural soil (6.21) > BionSoil® (4.75) > Pahokee peat (3.43) > Ohio Shale (3.18). The relationship between log $K_{F,oc}$ or log $K'_{F,oc}$ and log C/N ratio was presented in Fig. 3. The log $K_{F,oc}$ and log $K'_{F,oc}$ values decreased linearly with log C/N for both PHE and PYR.

3.1.4. Polanyi-Manes Model (PMM)

The nonlinear isotherm models, i.e., Polanyi−Manes was tested to fit the experimental data showed in Fig. 4. Application of PMM had the highest adjusted coefficient of determination (R^2) both for PHE and PYR (Table 3). The maximum sorption capacity q_{max} was calculated at equation (4), based on the fitting results using PMM (Table 3). The results indicated that PHE (PHE > PYR) was the maximum adsorbed in all sorbents compared to PYR. For PHE, the maximum sorption capacity (q_{max}) was in the order of 50% HDTMA-M 9.1 > Ohio Shale 2.7 > Pahokee peat 1.7> BionSoil® 1.1 > vermicompost 0.98 > natural soil 0.17. The order of decrease in the q_{max} value for sorption of PHE was consistent with the decrease in K'_F value (Table 2). For pyrene, the maximum sorption capacity (q_{max}) was in the order of 50% HDTMA-M 0.66 > Pahokee peat 0.49 > vermicompost 0.29 > BionSoil® 0.25 > Ohio Shale 0.24 >

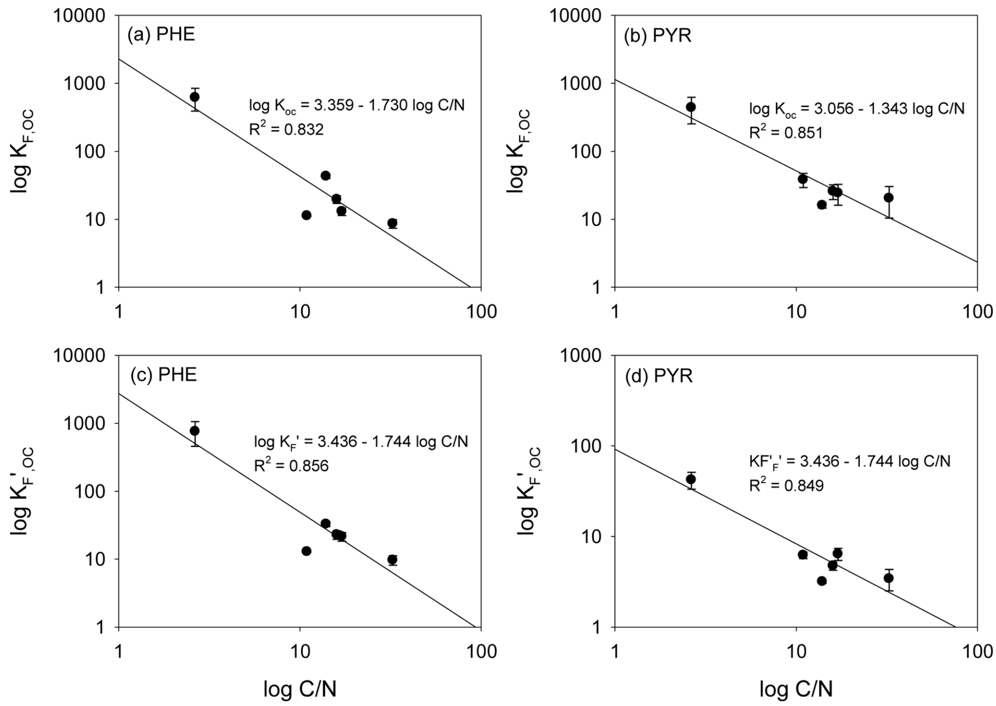

Fig. 3. Relationship between (a, b) log $K_{F,oc}$ and (c, d) $K'_{F,oc}$ vs. log C/N for sorption of Phenanthrene and pyrene in 50% HDTMA-M, Ohio Shale, Pahokee peat, BionSoil®, vermicompost and natural soil sorbents.

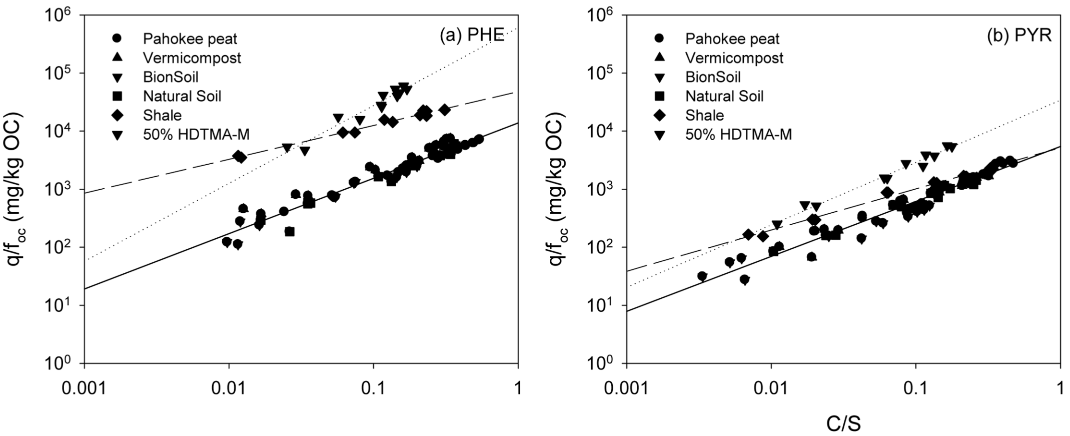

Fig. 4. Adsorption isotherms of phenanthrene and pyrene on several sorbents. The solid lines are the Polanyi−Manes (PMM) model fitting results.

Table 3. PMM parameters for sorption of phenanthrene and pyrene in sorbents

Sorbent	Solute	q_{max}	$q_{max,oc}$	α	R^2	SSE
Natural soil	PHE	0.1764 ± 0.006	7.84 ± 0.28	$2.06 \times 10^{-5} \pm 1.80 \times 10^{-6}$	0.9789	0.0010
	PYR	0.0808 ± 0.004	3.59 ± 0.18	$1.44 \times 10^{-5} \pm 1.62 \times 10^{-6}$	0.9641	0.0003
BionSoil®	PHE	1.1274 ± 0.107	10.14 ± 0.97	$1.61 \times 10^{-5} \pm 2.52 \times 10^{-6}$	0.9460	0.0708
	PYR	0.2516 ± 0.015	2.26 ± 0.14	$9.39 \times 10^{-6} \pm 1.03 \times 10^{-6}$	0.9628	0.0025
Pahokee peat	PHE	1.7126 ± 0.133	3.75 ± 0.29	$8.10 \times 10^{-6} \pm 8.99 \times 10^{-7}$	0.9585	0.0977
	PYR	0.4908 ± 0.072	1.07 ± 0.16	$7.07 \times 10^{-6} \pm 1.09 \times 10^{-6}$	0.9353	0.0072
Vermicompost	PHE	0.9829 ± 0.082	7.17 ± 0.60	$1.67 \times 10^{-5} \pm 2.52 \times 10^{-6}$	0.9408	0.0629
	PYR	0.2853 ± 0.021	2.08 ± 0.16	$8.92 \times 10^{-6} \pm 1.13 \times 10^{-6}$	0.9471	0.0036
Ohio Shale	PHE	2.6762 ± 0.130	27.65 ± 1.35	$6.43 \times 10^{-6} \pm 7.40 \times 10^{-7}$	0.9672	0.2487
	PYR	0.2444 ± 0.009	2.52 ± 0.10	$6.33 \times 10^{-6} \pm 4.89 \times 10^{-7}$	0.9843	0.0013
50% HDTMA-M	PHE	9.0632 ± 1.865	163.9 ± 33.74	$1.58 \times 10^{-5} \pm 2.54 \times 10^{-6}$	0.9284	1.2986
	PYR	0.6624 ± 0.084	11.98 ± 1.52	$1.12 \times 10^{-5} \pm 1.29 \times 10^{-6}$	0.9649	0.0055

Units: q_{max} = (mg/g) and $q_{max,oc}$ = (mg/g OC)

natural soil 0.08. The best fitting results of PMM were also observed by other researchers (Bui and Choi, 2010; Pan et al., 2008), who tested the sorption of organic contaminants with different properties by carbon materials. High values of R^2 for PMM suggest that in this case PMM seems not only applicable for pore filling but also applicable for surface adsorption (Yang et al., 2006).

3.2. Binary Sorption

Binary competitive sorption of PHE/PYR was conducted for natural soil only (Fig. 5). As expected, when two solutes are competing for sorption in the binary system, the sorption amount of each solute was reduced compared to that in a single-solute system. In order to determine the effect of binary competition on the degree of reduction quantitatively, the distribution coefficient (K_d) of the linear model in the binary system was analyzed. The partition coefficient, K_d, of each solute in single and binary systems and the percentage increase or decrease in K_d in the binary system are shown in Table S3. As the sorption affinity in the single-solute system is stronger (i.e., PYR > PHE), the reduction in K_d for the solute in the binary system becomes smaller (i.e., 16.6% < 25.2%). Competition between the solutes drives the weakly sorbed solute (PHE) to be desorbed from the sorbed phase, thereby allowing the stronger solute (PYR) to occupy larger sorption sites in natural soil (White et al., 1999).

The binary sorption isotherm of each solute was reduced

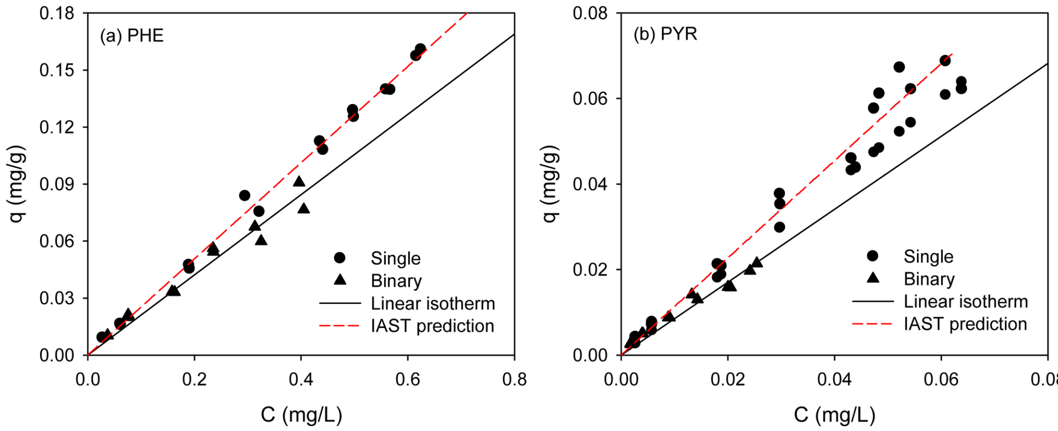

Fig. 5. Competitive sorption of phenanthrene and pyrene in natural soil. (a) Phenanthrene and (b) pyrene in PHE/PYR system, respectively. (Sorbent weight = 0.05 g).

compared to the single-solute sorption isotherm. The more hydrophobic PYR had a higher sorption affinity (as indicated by K_d) than the less hydrophobic PHE (Table S4). Generally, in binary sorption, the more hydrophobic HOC with a higher sorption affinity tends to be more desorption-resistant than less hydrophobic one (Table S4). For example, White et al. (1999) reported that more hydrophobic pyrene drives desorption of less hydrophobic phenanthrene in the competitive sorption. In this study, however, no difference between the two PAHs was observed.

IAST predictions for the binary competitive sorption were shown together in Fig. 5, for comparison. The binary predictive IAST used the single-solute sorption model, the parameters of which were previously determined from single-solute sorption (Table 2). In order to implement the IAST predictions, following functional relationships provided:

$$C^0_{m,2} = f(C^0_{m,1}) = g(q^0_{m,1}) \text{ and } q^0_{m,2} = h(q^0_{m,1}) \qquad (8)$$

where superscript 0 denotes initial concentration in the case of sorption. For the binary sorption protocol, i.e., the fixed weight of sorbent and the varying initial concentrations satisfying $C^0_{m,1} = C^0_{m,2}$, and the functional relationships become $C^0_{m,1} = C^0_{m,2}$ and $q^0_{m,1} = q^0_{m,2} = 0$ for the fresh sorbents. Equations 8-9 were used to compare the predictions of experimental data (Billemont et al., 2017) to calculate R^2 and SSE, as shown in Table S3.

$$R^2 = \frac{\sum q_i^2 - SSE}{\sum q_i^2} \qquad (9)$$

where

$$SSE = \sum (q_i - \tilde{q}_i)^2 \qquad (10)$$

In the equation (8), $\tilde{q}_i$ denotes the IAST-predicted uptake of a solute.

The predictions from the IAST are shown together with binary competitive sorption data for visual comparison (Fig. 5). To compare the performance of the IAST predictions with the binary sorption data, the R^2 and SSE values were computed and listed in Table S3 for the IAST predictions coupled to the single-solute Freundlich model. The R^2 values indicates that the IAST-Freundlich model (Table 2) were successful. However, the IAST predictions for the binary competitive sorption were nearly same as linear sorption isotherms. This illustrates that IAST was not successful in the prediction of hydrophobic organic compounds with low solubility, especially when the isotherms are almost linear (Qiao and Hu, 2000).

4. Conclusions

Sorption behaviors of PHE and PYR in natural and synthetic sorbents were investigated using single and binary systems. To characterize the sorption behaviors of PHE and PYR, four different models were used, i.e., linear, Freundlich, solubility-normalized Freundlich, and Polanyi-Manes. The linear model parameter (log K_{oc}) was well correlated with log C/N, whereas the Freundlich model parameters (log $K_{F,oc}$ and N_F) and the PMM parameter (log $q_{max,oc}$) were negatively correlated with log C/N. Competition between the solutes in binary sorption caused a reduction in the sorbent amount of each solute compared with that in the single-solute system. The IAST predictions for binary competitive sorption were nearly the same as for single-solute sorption. This illustrates that IAST was not successful in the prediction of hydrophobic organic compounds with low solubility, especially when the single-solute sorption isotherms are nearly linear.

Acknowledgements

This work was supported by Korea Environmental Industry & Technology Institute (KEITI) through Aquatic Ecosystem Conservation Research Program, funded by Korea Ministry of Environment (MOE) (No. 2021003040004)

References

Akinpelu, A.A., Ali, M.E., Johan, M.R., Saidur, R., Qurban, M.A., and Saleh, T.A., 2019, Polycyclic aromatic hydrocarbons extraction and removal from wastewater by carbon nanotubes: A review of the current technologies, challenges and prospects, *Process Saf. Environ. Prot*., **122**, 68-82. https://doi.org/10.1016/j.psep.2018.11.006

Al-Masud, M.A., Kim, D.G., and Shin, W.S., 2022a, Highly efficient degradation of phenolic compounds by Fe(II)-activated dual oxidant (persulfate/calcium peroxide) system, *Chemosphere*, **299**, 134392. https://doi.org/10.1016/j.chemosphere.2022.134392

Al-Masud, M.A., Shin, W.S., and Kim, D.G., 2023, Degradation of phenol by ball-milled activated carbon (AC_{BM}) activated dual oxidant (persulfate/calcium peroxide) system: Effect of preadsorption and sequential injection, *Chemosphere*, **312**, 137120. https://doi.org/10.1016/j.chemosphere.2022. 137120

Barriuso, E., Baer, U., and Calvet, R., 1992, Dissolved organic-matter and adsorption-desorption of dimefuron, atrazine, and carbetamide by soils, *J. Environ. Qual*., **21**(3), 359-367.

Billemont, P., Heymans, N., Normand, P., and De Weireld, G., 2017, IAST predictions vs co-adsorption measurements for CO_2 capture and separation on MIL-100 (Fe), *Adsorption*, **23**, 225-237. https://doi.org/10.1007/s10450-016-9825-6

Bui, T.X. and Choi, H., 2010, Comment on adsorption and desorption of oxytetracycline and carbamazepine by multi-walled carbon nanotubes, *Environ. Sci. Technol*., **44**(12), 4828. https://doi.org/10.1021/es100684f

Chen, Xian, Liang, J., Bao, L., Gu, X., Zha, S., and Chen, X., 2022, Competitive and cooperative sorption between triclosan and methyl triclosan on microplastics and soil, *Environ. Res*., **212**, 113548. https://doi.org/10.1016/j.envres.2022.113548

Choi, J. and Shin, W.S., 2020, Removal of salicylic and ibuprofen by hexadecyltrimethylammonium-modified montmorillonite and zeolite, *Minerals*, **10**(10), 898. https://doi.org/10.3390/min 10100898

Kim, J.-H., Shin, W.S., Song, D.-I., and Choi, S.J., 2005, Multi-step competitive sorption and desorption of chlorophenols in surfactant modified montmorillonite, *Water. Air. Soil Pollut*., **166**, 367-380. https://doi.org/10.1007/s11270-005-6329-5

Kim, Y.S., Song, D.I., Jeon, Y.W., and Choi, S.J., 1996, Adsorption of organic phenols onto hexadecyltrimethylammonium-treated montmorillonite, *Sep. Sci. Technol*., **31**(20), 2815-2830. https://doi.org/10.1080/01496399608000829

Kleineidam, S., Schüth, C., and Grathwohl, P., 2002, Solubility-normalized combined adsorption-partitioning sorption isotherms for organic pollutants, *Environ. Sci. Technol*., **36**(21), 4689-4697. https://doi.org/10.1021/es010293b

Krzyszczak, A., Dybowski, M.P., Zarzycki, R., Kobyłecki, R., Oleszczuk, P., and Czech, B., 2022, Long-term physical and chemical aging of biochar affected the amount and bioavailability of PAHs and their derivatives, *J. Hazard. Mater*., **440**, 129795. https://doi.org/10.1016/j.jhazmat.2022.129795

Luna, F.M.T., Oliveira Filho, A.N., Araújo, C.C.B., Azevedo, D.C.S., and Cavalcante, C.L., 2016. Adsorption of polycyclic aromatic hydrocarbons from heavy naphthenic oil using commercial activated carbons. 1. Fluid-Particle Studies, *Ind. Eng. Chem. Res.*, **55**(29), 8176-8183. https://doi.org/10.1021/acs.iecr.6b01059

Masud, M.A. Al, Kim, D.G., and Shin, W.S., 2022, Degradation of phenol using Fe(II)-activated CaO_2: effect of ball-milled activated carbon (AC_{BM}) addition, *Environ. Res*., **214**, 113882. https://doi.org/10.1016/j.envres.2022.113882

Niasar, H.S., Li, H., Kasanneni, T.V.R., Ray, M.B., and Xu, C.C., 2016, Surface amination of activated carbon and petroleum coke for the removal of naphthenic acids and treatment of oil sands process-affected water (OSPW), *Chem. Eng. J*., **293**, 189-199. https://doi.org/10.1016/j.cej.2016.02.062

Nyström, F., Nordqvist, K., Herrmann, I., Hedström, A., and Viklander, M., 2020, Removal of metals and hydrocarbons from stormwater using coagulation and flocculation, *Water Res*., **182**, 115919. https://doi.org/10.1016/j.watres.2020.115919

Oh, S., Kwak, M.Y., and Shin, W.S., 2009, Competitive sorption of lead and cadmium onto sediments, *Chem. Eng. J*., **152**(2-3), 376-388. https://doi.org/10.1016/j.cej.2009.04.061

Pan, B., Lin, D., Mashayekhi, H., and Xing, B., 2008, Adsorption and hysteresis of bisphenol A and 17α-ethinyl estradiol on carbon nanomaterials, *Environ. Sci. Technol*., **42**(15), 5480-5485. https://doi.org/10.1021/es8001184

Papageorgiou, S.K., Katsaros, F.K., Kouvelos, E.P., and Kanellopoulos, N.K., 2009, Prediction of binary adsorption isotherms of Cu^{2+}, Cd^{2+} and Pb^{2+} on calcium alginate beads from single adsorption data, *J. Hazard. Mater*., **162**(2-3), 1347-1354. https://doi.org/10.1016/j.jhazmat.2008.06.022

Pathak, S., Sakhiya, A.K., Anand, A., Pant, K.K., and Kaushal, P., 2022. A state-of-the-art review of various adsorption media employed for the removal of toxic Polycyclic aromatic hydrocarbons (PAHs): An approach towards a cleaner environment, *J. Water Process Eng*., **47**, 102674. https://doi.org/10.1016/j.jwpe.2022.102674

Qiao, S. and Hu, X., 2000. Use IAST with MPSD to predict binary adsorption kinetics on activated carbon, *AIChE J*., **46**(9), 1743-1752. https://doi.org/10.1002/aic.690460906

Shakya, A., Vithanage, M., and Agarwal, T., 2022, Influence of pyrolysis temperature on biochar properties and Cr(VI) adsorption from water with groundnut shell biochars: Mechanistic approach, *Environ. Res*., **215**, 114243. https://doi.org/10.1016/j.envres. 2022.114243

Shin, W.S. and Song, D.I., 2005. Solubility-normalized Freundlich isotherm for the prediction of sorption of phenols in HDTMA modified montmorillonite, *Geosci. J*., **9**, 249-259. https://doi.org/10.1007/BF02910585

Tran, H.N., You, S.-J., Hosseini-Bandegharaei, A., and Chao, H.-P., 2017, Mistakes and inconsistencies regarding adsorption of contaminants from aqueous solutions: A critical review, *Water Res*., **120**, 88-116. https://doi.org/10.1016/j.watres.2017.04.014

White, J.C., Hunter, M., Pignatello, J.J., and Alexander, M., 1999. Increase in bioavailability of aged phenanthrene in soils by competitive displacement with pyrene, *Environ. Toxicol. Chem*., **18**(8), 1728-1732. https://doi.org/10.1897/1551-5028(1999)018<1728:IIBOAP>2.3.CO;2

Yang, K., Zhu, L., and Xing, B., 2006, Adsorption of polycyclic aromatic hydrocarbons by carbon nanomaterials, *Environ. Sci. Technol*., **40**(6), 1855-1861. https://doi.org/10.1021/es052208w

Zhu, M., Yao, J., Dong, L., and Sun, J., 2016, Adsorption of naphthalene from aqueous solution onto fatty acid modified walnut shells, *Chemosphere*, **144**, 1639-1645. https://doi.org/10.1016/j.chemosphere.2015.10.050